nature portfolio

Peer Review File

A one-step fabrication of soft-magnetic high entropy alloy fiber with excellent strength and flexibility

Corresponding Author: Professor Wei-Ming Yang

This file contains all reviewer reports in order by version, followed by all author rebuttals in order by version.

Attachments originally included by the reviewers as part of their assessment can be found at the end of this file.

Version 0:

Reviewer comments:

Reviewer #1

(Remarks to the Author)

Reviewer #2

(Remarks to the Author)
Review of the manuscript entitled: A one-step fabricated soft magnetic high entropy alloy fiber with excellent strength and flexibility

The introduction highlights the significance of the research topic, identifies current limitations, and introduces HEAs as a promising solution to balance conflicting material properties. It outlines the relevance of soft magnetic fibres, such as Co-based and Fe-based amorphous and polycrystalline fibres, in technological applications like sensors, actuators, and electromagnetic shielding devices. This context effectively underscores the importance of developing materials that meet the demands of modern flexible electronics, making the research question timely and relevant.
The research problem is well-identified and focused on balancing mechanical properties (strength and plasticity) and magnetic properties (low coercivity) in micrometre-scale fibres.
The text provides a concise background on HEAs, highlighting their potential to overcome the trade-offs in traditional materials. It effectively uses specific examples, such as FeCoNiTaAl HEA and Fe26Co25Ni20Cu15Al13.1Ga0.9 HEA, to demonstrate the promising mechanical and magnetic properties of HEAs. This sets up a logical rationale for investigating HEAs in the context of soft magnetic fibres.
The introduction identifies a significant research gap: the limited investigation of soft magnetic HEAs in micron-diameter fibres compared to bulk materials, thin films, and powders. It effectively highlights the challenges associated with traditional casting and thermomechanical processing techniques, which are unsuitable for producing micro-diameter fibres with optimal properties.
The proposed use of an in-rotating-water spinning method with extremely high cooling rates is an innovative approach to fabricating HEA fibres with coarse-grained structures. This methodology section is well-aligned with the research objectives, offering a potential solution to achieving the desired balance of properties in soft magnetic fibres.
While the introduction hints at the potential of HEAs, it could benefit from a deeper scientific explanation of why these alloys are particularly suitable for balancing mechanical and magnetic properties. Elaborating on the underlying principles, such as the role of nanoscale coherent precipitates and dual-phase structures, would provide a more comprehensive understanding of HEAs' advantages. Furthermore the introduction section could more explicitly discuss the potential impact and practical applications of the research findings. Highlighting how these developments could advance technology in specific industries that would underscore the study's contribution to the field.
Improving the clarity and structure of certain sections could enhance readability and coherence. For example, rephrasing complex sentences and ensuring smooth transitions between ideas would improve the overall flow of the introduction, making it more engaging and easier to follow.
The detailed characterization of the microstructural evolution of high entropy alloy (HEA) fibers upon annealing is a strong aspect of the research. The introduction effectively employs multiple techniques, such as X-ray diffraction (XRD), electron backscatter diffraction (EBSD), transmission electron microscopy (TEM), and atom probe tomography (APT), to provide a

comprehensive understanding of the microstructure. This multifaceted approach is critical in elucidating how annealing affects the fibers' properties. For instance XRD reveals a transition from a face-centered cubic (FCC) structure to the presence of an L12 structure upon annealing, indicating phase evolution.
The detection of the L12 structure in annealed fibers, along with the calculation of lattice constants and lattice misfit, provides valuable insights into the material's properties. The low lattice mismatch suggests high coherency at interfaces, which is crucial for improving the strength-ductility synergy by facilitating dislocation mobility.
EBSD results indicate a slight increase in grain size after annealing, while TEM and APT analyses reveal the formation and distribution of Ta-rich phases and L12 precipitates. These findings are critical in understanding the mechanisms behind the enhanced mechanical properties observed in annealed fibers.
The identification of the Ta-rich phase through SAED and elemental analysis is well-supported by TEM and APT data. The consistency across different characterization techniques strengthens the validity of the results.
While the characterization data are extensive, the explanation of the underlying mechanisms driving microstructural changes could be more explicit. For instance, discussing how the formation of the L12 phase specifically contributes to mechanical property improvements would add some depth to the discussion.
The discussion could benefit from comparing the microstructural features of HEA fibers with conventional soft magnetic materials to highlight the unique advantages of HEAs. This would provide a clearer context for the significance of the observed microstructural evolution.
The description of figures and supplementary data could be more concise and integrated into the main text to enhance readability. For example, summarizing key observations from figures and discussing their implications would help streamline the narrative.
The use of Lorentz-TEM (LTEM) to observe magnetic domain structures provides a detailed view of the domain wall behavior in as-spun and annealed fibers. The analysis of domain wall motion and pinning effects elucidates how microstructural changes during annealing influence magnetic properties, especially Hc. The text explains the pinning effect of the Ta-rich phase in as-spun fibers and how the reduction in its size and the formation of coherent L12 precipitates after annealing contribute to lower Hc. The schematic illustrations further enhance understanding by visualizing these interactions. The model relating grain size to Hc provides a theoretical framework for understanding how grain coarsening during annealing affects coercivity. The text appropriately contrasts theoretical predictions with experimental observations, highlighting discrepancies and possible reasons.
While the text notes the stability of Ms, a more detailed discussion on the atomic interactions contributing to this stability, particularly among Fe, Co, and Ni atoms, would be beneficial.
Also more specific details related to Ltz-TEM analysis like defocus parameters should be provided unless I have omitted them in the text.
The section on the deformation mechanism of high entropy alloy (HEA) fibers provides a comprehensive examination of how microstructural changes influence strength and ductility.
The comparison between as-spun and annealed fibers, with emphasis on the roughness and dimple size, effectively illustrates the differences in ductility and fracture mechanisms.
The use of electron backscatter diffraction (EBSD) inverse pole figure (IPF) images and kernel average misorientation (KAM) maps provides a detailed view of grain orientation and dislocation density.
The use of transmission electron microscopy (TEM) and high-resolution TEM (HRTEM) to study microstructural features at a finer scale adds depth to the discussion. The identification of glissile and Lomer dislocations, sub-grain boundaries, and amorphous regions highlights the complex dislocation interactions and phase transformations occurring during deformation.
The section effectively contrasts the deformation mechanisms in as-spun and annealed fibers. The presence of massive dislocations and amorphous phase formation in as-spun fibers indicates enhanced plasticity, while twinning and 9R phase formation in annealed fibers suggest mechanisms contributing to increased strength.
The analysis of the L12 phase's role in strengthening annealed fibers through precipitation strengthening and its interaction with dislocations provides crucial insights into the mechanisms that enhance the mechanical properties of HEA fibers.
The role of deformation-induced amorphization in enhancing ductility is mentioned but could be expanded upon. Further discussion on how this transformation specifically impacts mechanical properties and how it compares to other HEA systems would add depth.

Overall it is a well-structured, detailed and interesting submission but perhaps it should be targeted at a slightly lower impact journal due to the lack of that novelty defining findings.

Reviewer #3

(Remarks to the Author)
Although there are significant publications in the field of high entropy alloys, this paper appears to have made some publication-worthy contributions to the field. The authors' strategy was to control the relationship between microstructure, magnetism and the mechanical strength such that coercivity is minimized and tensile strength is maximized. Consequently, soft magnetic fibers of Fe34Co29Ni29Al3Ta3Si2, with good tensile elongation, were produced by in-rotating-water spinning method.
To be suitable for publication, especially in Nature Communications, some improvements are needed.
• The authors seem to have missed the opportunity to discuss their work in view of another work that (perhaps) is the most closely related composition to theirs (DOI: 10.1016/j.intermet.2020.106801). In terms of the constituent elements, the key difference is the use of Ta in the present work. Discussion of the differences in the magnetic properties would have been very insightful.

• A statement on example of soft magnetic materials application in which the fibers can be used would be useful. In many applications, the fibers may still need to be consolidated which affects the resultant properties for a specific application.

• The authors wrote that the Ta-rich phase was substantially reduced or eliminated in the heat-treated samples, compared to the as-cast samples. How could such a change in composition not reflected in the magnetization? The magnetization (emu/g) should be the sum of magnetic moment from the magnetic phases in the materials, normalized by the mass of both magnetic and non-magnetic contents. Some explanation is needed.

• Please describe the direction of the applied magnetic field during magnetic hysteresis measurement: along vs. across the wire length?

• It would be helpful if the rationale for selecting this heat treatment condition were stated.

• It would also be helpful to understand why the authors have not discussed all the other samples made.

• Since the hysteresis plots were not saturated, saturation magnetization (Ms) should not be used. Consider M@10kOe.

• On the First line of the Microstructure analysis section: please identify the “small peak” with its 2theta position.

• Why is the discussion on the Role of the Ta-rich phase missing in the Deformation Mechanism section?

• There are some terms introduced without definition. For example, TEM and 3D-APT, etc.

• There are several typographical errors in the manuscript that need to be addressed. These are some examples:
o “reorganized” on page 4 should be “recognized”
o A sentence that started with “it” on page 4 should be “It”
o The indefinite article “an” in line 5 of the Result and Discussion section should be “a”
o First line of the Microstructure analysis section: “were” should be “was”
o The preposition “to” is missing in line 7 of First line of the Microstructure analysis section.
o On line 2 of the “Deformation mechanism” section, is “rational” the correct word?
o Please check these sentences:
Page 17: “To reduce the impact of the grip on the specimens, a layer of cardboard was covered.”
Page 18: The grain morphology of the samples was characterized via electron backscatter diffraction (EBSD) was performed in a SEM (Verios G4 UC, Thermo Fisher Scientific).

Version 1:

Reviewer comments:

Reviewer #1

(Remarks to the Author)
The submission has been revised extensively. The authors have responded well to all the comments and issues raised. The submission can be accepted for publication.

Reviewer #2

(Remarks to the Author)
I believe this article is ready for publication. However, I encourage the authors to proofread the manuscript for typographical errors. For instance, the word “seem” on line 76 should be deleted.

Regarding the role of the Ta-rich phase on magnetization, the atomic weight of Ta is significantly higher than that of the other elements. This difference should be reflected in the magnetic properties, particularly magnetization, if Ta forms an impurity phase. Nonetheless, I acknowledge the complexity of fully explaining changes in magnetic properties within such a multi-component system. Therefore, I recommend that the authors consider future work to better understand this phenomenon, as the current response may not capture the primary driving effect.

Responses to the Reviewers' Comments

Reviewer #1:

In "A one-step fabricated soft magnetic high entropy alloy fibre with excellent strength and flexibility" by Yan Ma et. al., the authors fabricated soft magnetic HEA alloy micron-sized wires with tailored mechanical properties which is quite impressive. **It is a well-executed study that makes a valuable contribution to the field of material science.** The author has provided a thorough explanation and rationale for the formation of $Fe_{34}Co_{29}Ni_{29}Al_3Ta_3Si_2$ high entropy alloy (HEA) fibre. **The research addresses a critical and underexplored problem** in synthesis of large micron-sized soft magnetic fibers, providing insights into dislocation proximity, plasticity, the domain wall pinning and coarsening of grains leading to the formation of low coercivity multicomponent flexible wires. **The results presented are clear and in logical manner, effectively supporting the stated hypotheses.**

The authors have **well described** the ***beneficial mechanisms of magnetization and mechanical properties of fabricated micron-sized HEA fibers carried out through magnetic and microstructure analyses***. Minor revisions are recommended to refine the manuscript which are as follows:

Thanks for the reviewer's recognition of the high quality of our work and strong support on the publication of the paper. We have further revised the paper according to the reviewer's suggestions.

Comment 1: In page 2, line no. 61, it has been written that the first introduction of high

entropy alloys (HEAs) was in **2002**, but it was in **2004** as per references mentioned. Ref [18] by Ma et. al. was on bulk metallic glasses only.

Response 1: Thanks for the reviewer's helpful comment. As suggested, "2002" has been replaced by "2004", and the Ref [18] by Ma et. al. was deleted **(line 65, page 3).**

Modifications: Page 3 lines 65: "*Since the first introduction of high entropy alloys (HEAs) in 2004*[16, 17]*, HEAs have become an innovative design concept that is promising to overcome the tradeoff between strength and plasticity*[18, 19, 20, 21, 22]*.*"

Comment 2: A point defect can pin magnetic domains (Magnetic domains and domain wall pinning in atomically thin $CrBr_3$ revealed by nanoscale imaging, Nature Communications, 12 (2021), 1989). Not pinning of magnetic wall domains by nanocrystalline $L1_2$ precipitates needs further scientific verifications and discussions. May be the coherency and not the size helped in the not-pinning process.

Response 2: Thanks for the reviewer's helpful comments. The authors fully agree with your insightful comment, and the discussion on pinning of magnetic wall domains by $L1_2$ precipitates has been added in the revised manuscript. In addition, we have cited the [Nature Communications, 12 (2021), 1989)] as Ref. 59 to discuss the effect of Ta-rich phase on pinning of domain walls in the revised manuscript.

The $CrBr_3$ is an ultra-thin single crystal with a thickness of ~2 nm. Therefore, magnetic domains are highly sensitive to defects, which alter the energy of the magnetic domain walls and hence affect domain wall motion [1]. However, for nanocrystalline/polycrystalline alloys, when the grain size is significantly smaller than

the domain wall thickness, these grains will not pin the domain wall motion. This is a common phenomenon in (Fe, Co)-based soft magnetic alloys [2]. In this work, the domain wall thickness of the as-spun and annealing HEA fibers is estimated to be 119 nm and 112 nm, respectively, while the grain sizes of the Ta-rich phase and $L1_2$ nanoprecipitates are approximately 310 nm and less than 20 nm, respectively. On one hand, the size of $L1_2$ nanoprecipitates in the annealed fibers is less than 20 nm (Fig. 2), which is far smaller than the domain wall width. On the other hand, the multiple coherent interfaces of FCC/$L1_2$, can significantly diminish the internal strain in the fibers, weakening the domain wall pinning by precipitates and phase boundary. [3] Therefore, the domain walls in FCC phase can be easily pulled out from these $L1_2$ nanoprecipitates, resulting in the low H_c, as demonstrated in Fig. 4b. **(lines 265-271, page 13).**

The $Ta_2(Co/Fe/Ni)_3Si$ particles, with size exceeding the critical domain wall width, will form and pin the domain wall movement [1] (arrow 1 in Fig.4a). However, the volume fraction of the particles in the as-spun HEA fibers is only 1.2%, thus having limited effect on increasing the H_c **(lines 245-248, page 12).**

Modifications: In the revised manuscript, we have added the following statement:

On Page 12 lines 244-248: "*Its size in FCC matrix reaches approximately 310 nm, which is larger than the domain wall width. Thus, the $Ta_2(Co/Fe/Ni)_3Si$ particles with size exceeding the critical domain wall width will form and pin the domain wall movement [59] (arrow 1 in Fig. 4a). However, the volume fraction of the particles in the as-spun HEA fibers is only 1.2%, thus having limited effect on increasing the H_c.*"

On Page 13 lines 265-271: "*On the one hand, the size of $L1_2$ nanoprecipitates in the*

annealed fibers is less than 20 nm (Fig. 2), which is far smaller than the domain wall width. On the other hand, the multiple coherent interfaces of FCC/$L1_2$, can greatly diminish the internal strain in the fibers, and weak the domain wall pinning by precipitates and phase boundary [13]. Therefore, the domain walls in FCC phase can be easily pulled out from these $L1_2$ nanoprecipitates, resulting in the low H_c, as demonstrated in Fig. 4b."

Comment 3: The readers would find it more relatable if the JCPDS data used for phase identification and peak matching in XRD were also mentioned.

Response 3: Thanks for the reviewer's suggestions. The diffraction peaks were identified based on FCC and $L1_2$ type structure by standard JCPDS (Card No. 65-5131 and 65-0140) data, respectively. The information has been added in the revised manuscript **(lines 431-434, page 21).**

Modifications: On Page 21 lines 431-434: "*Phase composition of the fibers was determined by X-ray diffraction (XRD, Burkle D8 Discover) with Cu-Kα radiation. The diffraction peaks were identified based on FCC and $L1_2$ type structure by standard JCPDS (Card No. 65-5131 and 65-0140) data, respectively.*"

Reviewer #2:

Review of the manuscript entitled: A one-step fabricated soft magnetic high entropy alloy fiber with excellent strength and flexibility.

Thanks for the reviewer's recognition and the positive comments on our paper. The reviewer's comments can be classified into four parts:

Part 1:

The introduction highlights the significance of the research topic, identifies current limitations, and introduces HEAs as a promising solution to balance conflicting material properties. It outlines the relevance of soft magnetic fibres, such as Co-based and Fe-based amorphous and polycrystalline fibres, in technological applications like sensors, actuators, and electromagnetic shielding devices. This context effectively underscores the importance of developing materials that meet the demands of modern flexible electronics, making the research question timely and relevant.

The research problem is **well-identified** and focused on balancing mechanical properties (strength and plasticity) and magnetic properties (low coercivity) in micrometre-scale fibres.

The text provides a concise background on HEAs, **highlighting their potential to overcome the trade-offs in traditional materials.** It effectively uses specific examples, such as FeCoNiTaAl HEA and $Fe_{26}Co_{25}Ni_{20}Cu_{15}Al1_{3.1}Ga_{0.9}$ HEA, to demonstrate the promising mechanical and magnetic properties of HEAs. This sets up a logical rationale for investigating HEAs in the context of soft magnetic fibres.

The introduction identifies a significant research gap: the limited investigation of

soft magnetic HEAs in micron-diameter fibres compared to bulk materials, thin films, and powders. It effectively highlights the challenges associated with traditional casting and thermomechanical processing techniques, which are unsuitable for producing micro-diameter fibres with optimal properties.

The proposed use of an in-rotating-water spinning method with extremely high cooling rates is **an innovative approach to fabricating HEA fibres with coarse-grained structures.** This methodology section is **well-aligned** with the research objectives, **offering a potential solution** to achieving the desired balance of properties in soft magnetic fibres.

Thanks for the reviewer's recognition of the high quality of our paper.

Comment 1: While the introduction hints at the potential of HEAs, it could benefit from a deeper scientific explanation of why these alloys are particularly suitable for balancing mechanical and magnetic properties. Elaborating on the underlying principles, such as the role of nanoscale coherent precipitates and dual-phase structures, would provide a more comprehensive understanding of HEAs' advantages. Furthermore, the introduction section could more explicitly discuss the potential impact and practical applications of the research findings. Highlighting how these developments could advance technology in specific industries that would underscore the study's contribution to the field.

Response 1: Thanks for the reviewer's helpful comments and suggestions.

The most widely adapted soft magnetic materials, including silicon steel, permalloy and amorphous alloy, can be strengthened by dislocation, second phase and

grain boundary etc. [4], which may severely deteriorate plasticity and H_c. Meanwhile, improving H_c of aforementioned magnetic alloys also requires alleviating stress and lattice distortion via annealing, which leads to aging effects and annealing brittleness [5]. For HEAs, nanoscale coherent precipitates have been introduced to improve both strength and plasticity. When dislocations cut through these coherent precipitates, mechanical strength is enhanced by the precipitates and strong bonding of different atoms [6]. Compared with randomly structured segregation, the inconspicuous misfit between coherent nanoprecipitates and matrix could also alleviate stress concentration, effectively balancing strength and plasticity. In the meantime, the full coherency between nanoprecipitates and matrix doesn't hinder domain wall movement, leading to a low H_c [7]. Therefore, the HEAs are particularly suitable for balancing mechanical and magnetic properties.

In response to the comment 1, we have made corresponding supplements and modifications in the Introduction, as follows:

Recently, permalloys and Co/Fe-based SMFs have obtained significant attention owing to their potential applications in geomagnetic navigation, human-computer interaction, and human-like tactile sensing. However, their limited stretchability poses numerous challenges for the large-scale production and application [8].

Since the introduction of high entropy alloys (HEAs) in 2004 [9, 10], HEAs have emerged as a promising design concept to balance strength and plasticity [11, 12, 13, 14, 15]. In addition to extensive research on their mechanical properties, there has been a growing interest in their soft magnetic properties [16, 17, 18]. For instance, the bulk

FeCoNiTaAl HEA with nanoscale coherent precipitates exhibits a tensile strength of 1336 MPa at 54% tensile elongation, a low H_c of 78 A/m, and a moderate saturation magnetization (M_s) of 1.10 T [6, 7]. The dual-phase $Fe_{26}Co_{25}Ni_{20}Cu_{15}Al_{13.1}Ga_{0.9}$ HEA with coherent nanoprecipitates balances compressive strength (1448 MPa), strain (200 %), and H_c (4.19 Oe) [3]. The single-phase $(Co_{30}Fe_{45}Ni_{25})_{0.8}(Al_{40}Si_{60})_{0.2}$ HEA has a combination of high yielding strength of 1636 MPa, relatively-high M_s of 1.24 T, and low H_c of 0.75 Oe [19] . It is suggested that HEAs can optimize plasticity and H_c by tuning particle/matrix interfacial coherency stresses to maximize interaction strength with dislocations and minimize magnetic pinning of domain walls [6].

For crystalline soft magnetic alloys ($FeSi_{6.5}$, $Fe_{50}Ni_{50}$, etc), when the grain size is between 1 μm and 1 mm, the H_c decreases with grain coarsening, satisfying the relationship as $H_c \propto 1/D$ (D is the grain size) [20]. Also, coarse-grained structure is usually beneficial to plasticity [21]. In this work, an in-rotating-water spinning method was first used to achieve micron-diameter SMFs with coarse-grained structure through a short production line, representing an energy-saving and high-efficiency process [22, 23]. The metalloid element Si was introduced into the Fe-Co-Ni-Al-Ta system to suppress the pinning effects of Ta and effectively improve the plasticity without deteriorating coercivity [24, 25].

This work thus ensures the compatibility of mechanical and soft magnetic properties of SMFs under multi-dimensional deformations and high temperatures, facilitating their large-scale production and application in emerging fields such as wearable electronics, humanoid robots, and intelligent construction.

Modifications: On Page 3 lines 51-56: "*Recently, permalloys and Co/Fe-based SMFs have obtained significant attention owing to their potential applications in geomagnetic navigation, human-computer interaction, and human-like tactile sensing. However, due to limited stretchability, the large-scale production and application of SMFs and related devices still face numerous challenges*[8]."

On Page 4 lines 74-79: "*The single-phase* $(Co_{30}Fe_{45}Ni_{25})_{0.8}(Al_{40}Si_{60})_{0.2}$ *HEA has a combination of high compressive strength of 1636 MPa, relatively-high* M_s *of 1.24 T, and low* H_c *of 0.75 Oe* [26]*. It seems that HEAs with high structural disorder, designable crystal structure and variable magnetic properties can balance plasticity and* H_c *by tuning particle/matrix interfacial coherency stresses to maximize the interaction strength with dislocations and minimize the pinning of magnetic domain walls* [11]."

On Page 5 lines 92-94: "*In this work, an in-rotating-water spinning method was first used to achieve micron-diameter SMFs with coarse-grained structure through a short, energy-saving and high-efficiency process*[34, 35]."

On Page 5 lines 99-103: "*This work thus ensures the compatibility of mechanical and soft magnetic properties of SMFs under multi-dimensional deformations and high temperatures, facilitating their large-scale production and application in emerging fields such as wearable electronics, humanoid robots, and intelligent construction.*"

On Page 19 lines 382-384: "*In conclusion, micron-scale SMFs with excellent strength and flexibility have been successfully achieved via Si microalloying and one-step in-rotating-water spinning method in the Fe-Co-Ni-Al-Ta HEA.*"

Comment 2: Improving the clarity and structure of certain sections could enhance

readability and coherence. For example, rephrasing complex sentences and ensuring smooth transitions between ideas would improve the overall flow of the introduction, making it more engaging and easier to follow.

Response 2: Considering the reviewer's suggestions, the English grammar and the expressions were checked point by point to avoid mistakes by authors. Besides, our good English colleagues have also helped us checking and editing the language of full manuscript.

Part 2:

The detailed characterization of the microstructural evolution of high entropy alloy (HEA) fibers upon annealing is **a strong aspect of the research**. The introduction effectively employs multiple techniques, such as X-ray diffraction (XRD), electron backscatter diffraction (EBSD), transmission electron microscopy (TEM), and atom probe tomography (APT), to **provide a comprehensive understanding** of the microstructure. This multifaceted approach is critical in elucidating how annealing affects the fibers' properties. For instance XRD reveals a transition from a face-centered cubic (FCC) structure to the presence of an $L1_2$ structure upon annealing, indicating phase evolution.

The detection of the $L1_2$ structure in annealed fibers, along with the calculation of lattice constants and lattice misfit, **provides valuable insights into the material's properties**. The low lattice mismatch suggests high coherency at interfaces, which is crucial for improving the strength-ductility synergy by facilitating dislocation mobility. EBSD results indicate a slight increase in grain size after annealing, while TEM and

APT analyses reveal the formation and distribution of Ta-rich phases and $L1_2$ precipitates. **These findings are critical in understanding the mechanisms behind the enhanced mechanical properties observed in annealed fibers.**

The identification of the Ta-rich phase through SAED and elemental analysis is **well-supported by TEM and APT data**. The consistency across different characterization techniques **strengthens the validity of the results**.

Thanks for the reviewer's recognition of the high quality of our paper.

Comment 3: While the characterization data are extensive, the explanation of the underlying mechanisms driving microstructural changes could be more explicit. For instance, discussing how the formation of the $L1_2$ phase specifically contributes to mechanical property improvements would add some depth to the discussion.

Response 3: The authors agree to your insightful comment, the discussion on microstructure-property relationship has been expanded in the revised manuscript **(lines 199-209, page 10).**

Introducing nanoscale $L1_2$ phase has recently been proven to be an effective precipitation strengthening method in FCC HEAs [26, 27, 28]. The APT data in Fig. 3f reveals the enrichment of Ni (50.2 at.%), Al (11.6 at.%) and Ta (11.2 at.%), whose concentrations are much higher than those in the alloy matrix (29 at.% Ni, 3 at.% Al and 3 at.% Ta). Al can act as a strong $L1_2$ former in Ni/Co containing HEAs [29], while the addition of Ta promotes the continuous precipitation of $L1_2$ particles [30]. Since the ordered $L1_2$ precipitates are much stronger than the FCC solid solution matrix, higher stresses are thus required for dislocations in matrix to cut through the $L1_2$ precipitates,

which leads to the significant improvement of strength (Fig. 1e). These nanosized hard particles dispersed in matrix also degenerate the dislocation storage ability by reducing the mean free path of dislocations and give rise to the decreased ductility (Fig. 1e).

Modifications: In the revised manuscript, we have added the following discussion to address these points on Page 10 lines 199-209:

"*Introducing nanoscale $L1_2$ phases has recently been proven to be an effective precipitation strengthening method in FCC HEAs*[51, 52, 53]*. The profiles in Fig. 3f reveals the enrichment of Ni (50.2 at.%), Al (11.6 at.%) and Ta (11.2 at.%), whose concentrations are much higher than those in the alloy matrix (29 at.% Ni, 3 at.% Al and 3 at.% Ta). Al can act as a strong $L1_2$ former in Ni/Co containing HEAs*[54]*, while the addition of Ta promotes the continuous precipitation of $L1_2$ particles*[55]*. Since the ordered $L1_2$ precipitates are much stronger than the FCC solid solution matrix, higher stresses are thus required for dislocations in matrix to cut through the $L1_2$ precipitates, which leads to the significant improvement of strength (Fig. 1e). These nanosized hard particles dispersed in matrix also degenerate the dislocation storage ability by reducing the mean free path of dislocations, thus giving rise to the decreased plasticity (Fig. 1e).*"

Comment 4: The discussion could benefit from comparing the microstructural features of HEA fibers with conventional soft magnetic materials to highlight the unique advantages of HEAs. This would provide a clearer context for the significance of the observed microstructural evolution.

Response 4: The authors totally agree to your insightful comment, and the discussion on comparing the microstructural features of HEA fibers with conventional soft

magnetic materials has been expanded in the revised manuscript.

The most widely adapted soft magnetic materials, including silicon steel, permalloy and amorphous alloy, can be strengthened by dislocation, second phase and grain boundary etc. [4], which may deteriorate plasticity and H_c severely. Meanwhile, improving H_c of aforementioned magnetic alloys also requires alleviation of stress and lattice distortion via annealing, which leads to aging effects and annealing brittleness [5]. For HEAs, nanoscale coherent precipitates have been introduced to improve the strength and plasticity. When dislocation cuts the coherent precipitates, mechanical strength is enhanced by the precipitates and strong bonding of different atoms [6]. Compared with randomly structured segregation, the inconspicuous misfit between coherent nanoprecipitates and matrix could also alleviate stress concentration, and balance strength and plasticity effectively. In the meantime, the full coherency between nanoprecipitates and matrix doesn't hinder domain wall movement, leading to a low H_c [7]. Therefore, the HEAs are particularly suitable for balancing mechanical and magnetic properties.

For crystalline soft magnetic alloys ($FeSi_{6.5}$, $Fe_{50}Ni_{50}$, etc), when the grain size is between 1 μm and 1 mm, the H_c decreases with grain coarsening, satisfying the relationship as $H_c \propto 1/D$ (D is the grain size) [20]. Also, coarse-grained structure is usually beneficial to plasticity [21]. The HEAs with high structural disorder, designable crystal structure and variable magnetic properties can balance plasticity and H_c by tuning particle/matrix interfacial coherency stresses to maximize interaction strength with dislocations and minimize magnetic pinning of domain walls [6]. **(lines 92-94, page 5).**

On the one hand, the size of $L1_2$ nanoprecipitates in the annealed fibers is less than 20 nm (Fig. 2), which is far smaller than the domain wall width. On the other hand, the multiple coherent interfaces of FCC/$L1_2$, can greatly diminish the internal strain in the fibers, weaken the domain wall pinning by precipitates and phase boundary. [3] Therefore, the domain walls in FCC phase can be easily pulled out from these $L1_2$ nanoprecipitates, resulting in the low H_c, as demonstrated in Fig. 4b. **(lines 267-271, page 13).**

The slightly larger H_c of the as-spun fibers compared to previously reported $(Co_{30}Fe_{45}Ni_{25})_{1-x}(Al_{40}Si_{60})_x$ bulk HEAs is due to the pinning effect of the Ta-rich phase on the movement of the domain wall and the influence of localized stress [19]. The 800 ℃-120 min annealed fibers have a lower H_c owing to the cooperative effect of stress relaxation, the disappearance of Ta-rich phase, and the formation of $L1_2$ coherent nanoprecipitates. **(lines 274-276, page 13-14).**

It indicates that dislocation nucleation, multiplication, and motion are more readily activated in the as-spun fibers which possesses a larger plasticity. **(lines 308-310, page 15).**

The increase in strength is mainly attributed to the precipitation strengthening effect provided by the high-volume fraction of $L1_2$ particles. Region i in Fig. 5h is enlarged in Fig. 5i, along with its GPA strain map provided below the HRTEM image. It was observed in the GPA map that the PB is effective in blocking dislocations and thus contributes to strengthening. **(lines 358-362, page 18).**

Modifications: In the revised manuscript, we have included the following statements to comparing the microstructural features of HEA fibers with conventional soft

magnetic materials:

On Page 5 lines 92-94: "*In this work, an in-rotating-water spinning method was first used to achieve micron-diameter SMFs with coarse-grained structure through a short, energy-saving and high-efficiency process*[34, 35]."

On Page 13 lines 267-271: "*On the one hand, the size of $L1_2$ nanoprecipitates in the annealed fibers is less than 20 nm (Fig. 2), which is far smaller than the domain wall width. On the other hand, the multiple coherent interfaces of FCC/$L1_2$, can greatly diminish the internal strain in the fibers, and weak the domain wall pinning by precipitates and phase boundary*[13]*. Therefore, the domain walls in FCC phase can be easily pulled out from these $L1_2$ nanoprecipitates, resulting in the low H_c, as demonstrated in Fig. 4b.*"

On Page 13-14 lines 274-276: "*The slightly larger H_c of the as-spun fibers compared to previously reported $(Co_{30}Fe_{45}Ni_{25})_{1-x}(Al_{40}Si_{60})_x$ bulk HEAs is due to the pinning effect of the Ta-rich phase on the movement of the domain wall and the influence of localized stress*[26]."

On Page 15 lines 308-310: "*These phenomena indicate that dislocation nucleation, multiplication, and motion are more readily activated in the as-spun fibers, therefore possessing a larger plasticity.*"

On Page 18 lines 358-362: "*The increase in strength is mainly attributed to the precipitation strengthening effect provided by the high-volume fraction of $L1_2$ particles. Region i in Fig. 5h is enlarged in Fig. 5i, along with its geometric phase analysis (GPA) strain map provided below the HRTEM image. It was observed in the GPA map that the*

PB is effective in blocking dislocations and thus contributes to strengthening."

Comment 5: The description of figures and supplementary data could be more concise and integrated into the main text to enhance readability. For example, summarizing key observations from figures and discussing their implications would help streamline the narrative.

Response 5: Thanks for the reviewer's helpful comments. Based on the reviewers' comments, we improved Figure 2， redraw and added Figure 3. The narrative of the paper was simplified, and the readability was improved **(lines 166-219, page 8 ~ page 11).**

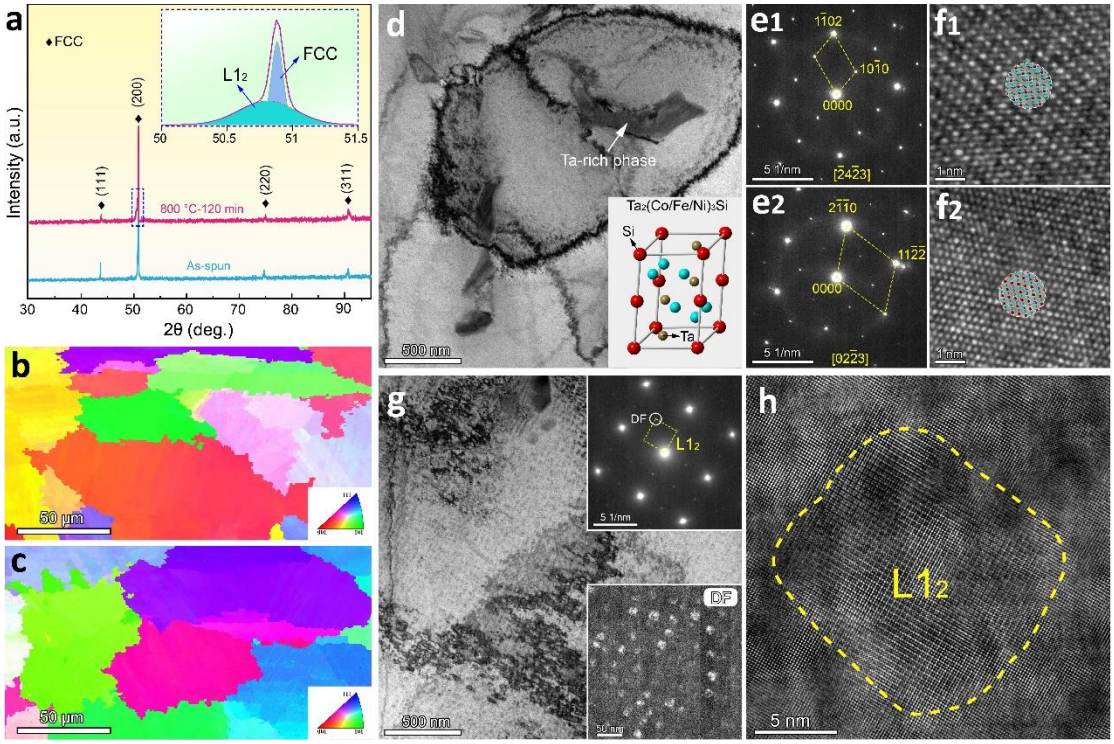

Figure 2 Microstructural evolution of HEA fibers. a XRD patterns of HEA fibers (Insert is the deconvolution of the diffraction peak of the HEA fibers). EBSD-IPF maps of **b** as-spun and **c** 800 °C-120 min annealed HEA fibers. **d** BF TEM image of as-spun HEA fibers, showing a Ta-rich phase in the FCC matrix. **e** SAED images taken along different zone axes of the Ta-rich phase and **f** their corresponding HRTEM images. The Ta-rich phase was identified to be $Ta_2(Co/Fe/Ni)_3Si$ according to the SAED patterns, as illustrated in the inset of **d**. **g** BF-TEM image of 800 °C-120 min annealed HEA fibers. The upper and lower insets of **g** are the corresponding SAED and DF-TEM images,

respectively. **i** HRTEM image showing a $L1_2$ nanoprecipitate.

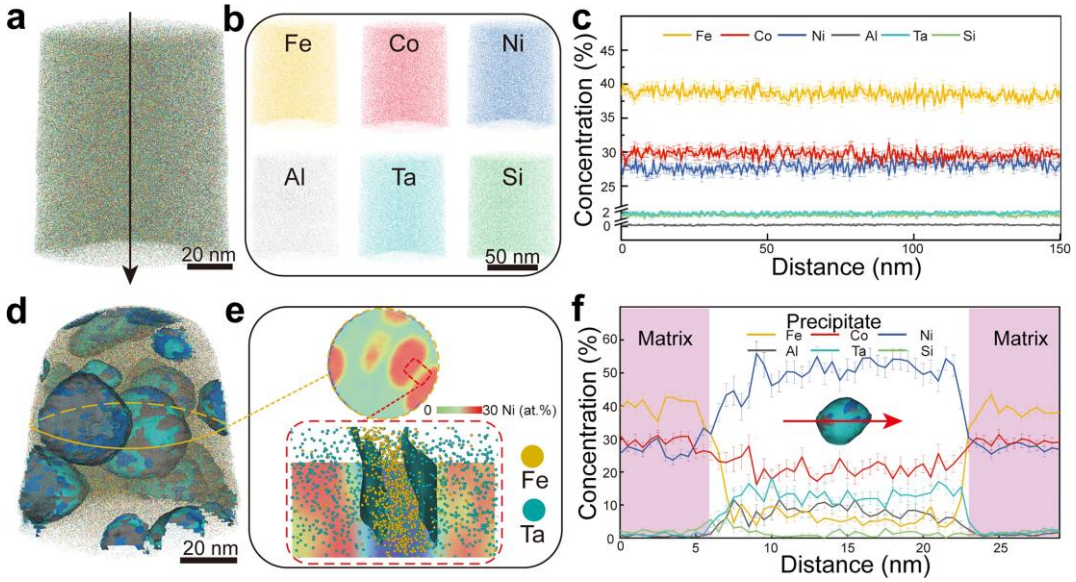

Figure 3 3D-APT maps of HEA fibers. a 3D-APT map of as-spun HEA fibers. b The uniform distribution of all elements in near atomic-scale in **a**. **c** 1D compositional profiles across the tip with the direction marked by the dark arrow in **a**. **d** 3D-APT map of 800 ℃-120 min annealed HEA fibers. **e** 2D projection of the Ni concentration slice acquired from the central part of the APT tip shown in **d** and enlarged view of the groove region showing the distribution of Fe and Ta atoms. **f** 1D compositional profiles showing the compositional changes across a selected precipitate along the red arrow shown in the inset. Error bars in **c** and **f** refer to the standard deviations of data points.

Modifications: In the revised manuscript, we have added the following discussion to further illustrate these two images:

On Page 8 lines 166-173: "*After annealed at 800 ℃ for 120 min, the $L1_2$ precipitates with an average size of 18 ± 2 nm were detected as indicated by the SAED and dark-field (DF) TEM images inserted in Fig. 2g. Compared with the as-spun state (Fig. 2d), the content of Ta-rich phase is obviously reduced or even disappeared. The HRTEM image in Fig. 2h confirms the ordered $L1_2$ phase (outlined by dotted yellow line) which shows full coherency with matrix lattice. The $L1_2$ phase has a near-spherical structure, which is related to the interfacial free energy of the particles[50]. It is mainly composed of Ta, Al and Ni elements (Supplementary Fig. S5b).*"

On Page 9-10 lines 187-197: "*Fig. 3d visualizes the near-spherical $L1_2$ nanoprecipitates in terms of a 3D reconstruction of a typical APT tip for the 800 ℃-120 min annealed sample. Fig. 3e provides a cross-sectional two-dimensional (2D) concentration plot in terms of a 30 at% Ni threshold value, acquired from the center region of the APT tip (Fig. 3d). From Fig. 3e, we selected two representative precipitate/matrix interfaces for further characterization (red dashed square). These results evidence Ni enrichment in the precipitates and Fe enrichment in the matrix, respectively. Fig. 3f shows 1D compositional profiles acquired across a selected precipitate (see red arrow in the inset of Fig. 3f). The chemical compositions of the FCC and the $L1_2$ phases were derived and averaged from several APT sub-volumes (Fig. S7).*"

Part 3:

The use of Lorentz-TEM (LTEM) to observe magnetic domain structures **provides a detailed view** of the domain wall behavior in as-spun and annealed fibers. The analysis of domain wall motion and pinning effects elucidates how microstructural changes during annealing influence magnetic properties, especially Hc. The text explains the pinning effect of the Ta-rich phase in as-spun fibers and how the reduction in its size and the formation of coherent L12 precipitates after annealing contribute to lower Hc. The schematic illustrations further enhance understanding by visualizing these interactions. The model relating grain size to Hc provides a theoretical framework for understanding how grain coarsening during annealing affects coercivity. **The text appropriately contrasts theoretical predictions with experimental observations,**

highlighting discrepancies and possible reasons.

Thanks for the reviewer's recognition of our paper.

Comment 6: While the text notes the stability of *M*s, a more detailed discussion on the atomic interactions contributing to this stability, particularly among Fe, Co, and Ni atoms, would be beneficial.

Response 6: Thanks for the reviewer's suggestions. A more detailed discussion on the atomic interactions contributing to the stability of M_s was added in the revised manuscript **(lines 221-227, page 11).**

Modifications: On page 11 lines 221-227: "*The magnetization and H_c are the key parameters of soft magnetic materials [56].The vacancies in 3d atomic orbitals of Fe, Co and Ni atoms contribute to the magnetic moments, and these vacancies will be filled up by the outer shell electrons of Al and Si[57]. The samples exhibit a stable magnetization at 10 kOe (Supplementary Fig. S2) owing to the magnetic exchange interaction from certain atomic ratio. Upon different annealing conditions, the Ta-rich phase occupies only a small fraction (<1.2%), thus having a negligible effect on magnetization.*"

Comment 7: Also more specific details related to Ltz-TEM analysis like defocus parameters should be provided unless I have omitted them in the text.

Response 7: Thanks for the reviewer's good suggestions. The defocus parameters of Ltz-TEM were added in revised manuscript **(lines 441-445, page 21-22).**

In-situ dynamic observation of magnetic viscosity was performed using Lorentz transmission electron microscopy (LTEM) (JEM-2100F) and a self-made horizontal magnetic in-situ sample holder. In focus distance, over focus distance and under focus

distance are -1.29 mm, -380 µm, and -2.21 mm, respectively. The Fresnel mode with a defocus of ~920 µm was used for observation.

Modifications: In our revised manuscript, we added the following statement on Page 21-22 lines 441-445:

"*In-situ dynamic observation of magnetic viscosity was performed using Lorentz transmission electron microscopy (LTEM) and a self-made horizontal magnetic in-situ sample holder. In focus distance, over focus distance and under focus distance are -1.29 mm, -380 µm and -2.21 mm, respectively. The Fresnel mode with a defocus of ~920 µm was used for observation.*"

Part 4:

The section on the deformation mechanism of high entropy alloy (HEA) fibers **provides a comprehensive examination** of how microstructural changes influence strength and ductility.

The comparison between as-spun and annealed fibers, with emphasis on the roughness and dimple size, effectively illustrates the differences in ductility and fracture mechanisms.

The use of electron backscatter diffraction (EBSD) inverse pole figure (IPF) images and kernel average misorientation (KAM) maps **provides a detailed view** of grain orientation and dislocation density.

The use of transmission electron microscopy (TEM) and high-resolution TEM (HRTEM) to study microstructural features at a finer scale adds depth to the discussion. The identification of glissile and Lomer dislocations, sub-grain boundaries, and

amorphous regions highlights the complex dislocation interactions and phase transformations occurring during deformation.

The section effectively contrasts the deformation mechanisms in as-spun and annealed fibers. The presence of massive dislocations and amorphous phase formation in as-spun fibers indicates enhanced plasticity, while twinning and 9R phase formation in annealed fibers suggest mechanisms contributing to increased strength.

The analysis of the L12 phase's role in strengthening annealed fibers through precipitation strengthening and its interaction with dislocations **provides crucial insights into the mechanisms** that enhance the mechanical properties of HEA fibers.

Thanks for the reviewer's recognition of the high quality of our paper.

Comment 8: The role of deformation-induced amorphization in enhancing ductility is mentioned but could be expanded upon. Further discussion on how this transformation specifically impacts mechanical properties and how it compares to other HEA systems would add depth.

Response 8: Thanks to your valuable comment. We have deepened the discussion by considering the role of amorphization in mechanical properties, and the comparison of the transformation with other HEAs has also been made in the revised manuscript **(lines 322-341, page 16-17).**

First of all, we would like to stress that the primary carrier of plasticity during the deformation of the as-spun HEA fibers is dislocation slip. Solid state amorphization generally occurs as a complementary/alternative deformation mechanism in scenarios where dislocation activities are suppressed or insufficient to accommodate the imposed

strain, such as in metallic materials subjecting to deformation at ultra-high strain rates[32, 33] or low temperature[34], in metals with nanocrystalline structures[35], and also in covalently-bonded solids [36, 37].

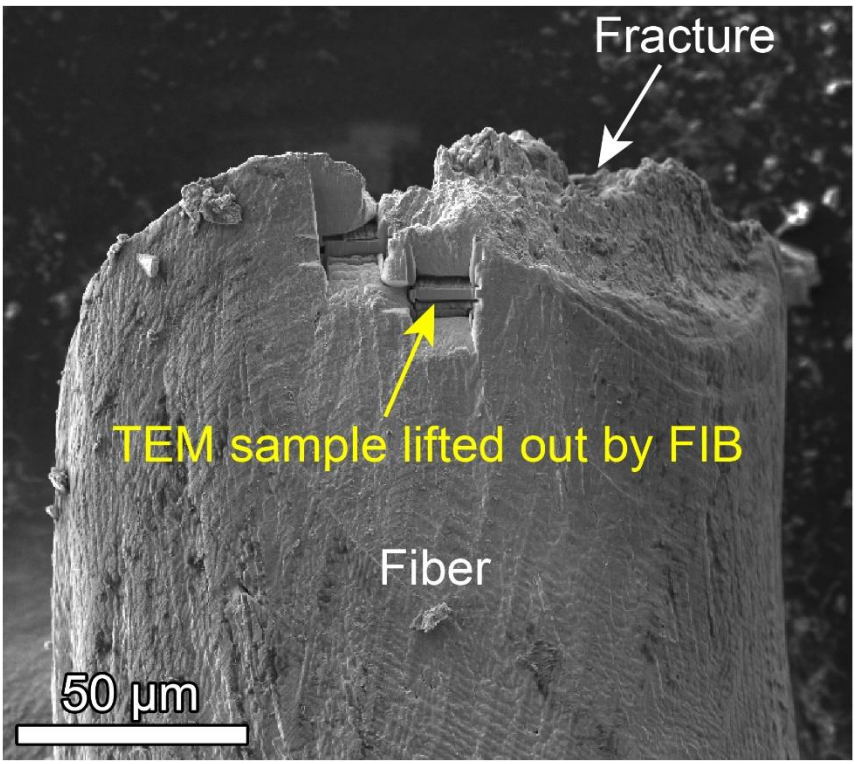

Figure R1. SEM image showing the location where TEM sample observed in Figure 4a was lifted out by FIB.

As a specific deformation mechanism, crystalline-to-amorphous transformation itself can contribute to ductility by introducing plastic strain which stems from the volume change and shear band development[38]. Moreover, compared to its crystalline counterpart, amorphous phase is at a higher energy state where extra energy is required during the crystal-to-amorphous transformation. The consumption of extra energy shall inhibit the initiation of micro-cracks by alleviating stress concentration at the intersections of dislocations and thus contribute to ductility[39]. Deformation-induced

amorphization has been reported in HEAs like FCC structured FeCoCrNi[40], CrMnFeCoNi[33, 34, 39] and $Al_{0.1}$CoCrFeNi[41], which is originated from significant dislocation accumulations and severe interactions among dislocations, twins and stacking faults. A recent study on BCC structured TiHfZrNb system HEAs has revealed that amorphization can even take place in elastic regime due to a large elastic strain (~10%)[42]. The observation in Fig. 5a was conducted on a TEM sample lifted out from the region near the fracture of the fiber using a FIB machine (Fig. R1), where severe plastic deformation occurs as testified by KAM maps in Fig. 5a and abundant dislocations in Fig. 5c. Therefore, the amorphization in the as-spun HEA fibers should be due to dislocation accumulations near the fracture.

Modifications: In our revised manuscript, we added the following discussions on Page 16-17 lines 322-341:

"*Deformation induced amorphization generally occurs as a complementary/alternative deformation mechanism in scenarios where dislocation activities are suppressed or insufficient to accommodate the imposed strain[63, 64, 65, 66, 67, 68]. As a specific deformation mechanism, amorphization itself can contribute to plasticity by introducing plastic strain which stems from the volume change and shear band development[69]. Moreover, compared to its crystalline counterpart, amorphous structure is at a higher energy state where extra energy is required during the crystal-to-amorphous transformation. The consumption of extra energy shall inhibit the initiation of micro-cracks by alleviating stress concentration at the intersections of dislocations and thus contribute to ductility[70]. Deformation-induced amorphization has also been reported in other HEAs like FCC*

structured FeCoCrNi[71], CrMnFeCoNi[63, 65, 70] and Al0.1CoCrFeNi[72], which is originated from significant accumulations and severe interactions of dislocations, twins and stacking faults. A recent study on BCC structured TiHfZrNb system HEAs has revealed that amorphization can even take place in elastic regime due to a large elastic strain (~10%)[73]. The observation in Fig. 5a was conducted on a TEM sample lifted out from the region near the fracture of the fiber using a FIB machine, where severe plastic deformation occurs as testified by KAM maps in Fig. 5a and abundant dislocations in Fig. 5c. Therefore, the amorphization in the as-spun HEA fibers should be due to dislocation accumulations near the fracture."

Comment 9: Overall **it is a well-structured, detailed and interesting submission** but perhaps it should be targeted at a slightly lower impact journal due to the lack of that novelty defining findings.

Response 9: Thanks for the reviewer's recognition of the high quality of our paper. Based on the reviewer's comment, we further revised and improved the paper to highlight the innovation points, justifying the publication of the paper in Nature Communications. As presented above, we have carefully addressed all the questions proposed by the reviewer. The innovation clarified in the revised manuscript mainly includes the following three points:

(1) Existing research on soft magnetic HEAs is mainly limited to bulk, thin films, and powders. Further, HEA fibers typically require multi-step processes such as casting, rolling, and drawing, which are energy-intensive and involve lengthy procedures, resulting in small grain sizes. In this work, a **one-step in-rotating-water spinning**

method was first used to achieve micron-diameter soft-magnetic HEA fibers with coarse-grained structure through a short production line, which corresponds to an energy-saving and high-efficiency process.

(2) Rapid cooling technique was used to suppress Ta-rich phase precipitation in HEA fibers, surprisingly **balancing the mechanical properties and soft magnetic properties of the fibers**. **The tensile elongation of the HEA fibers in our work outperforms all other SMFs, and the H_c of the HEA fibers is lower than that of FeCo, FeSi**, and metal deposited carbon fibers etc.【The content of Ta-rich phase as shown in Figure 1 and Figure S5 in the HEA fibers was significantly lower than that in the samples solidified near equilibrium (Figure R2).】

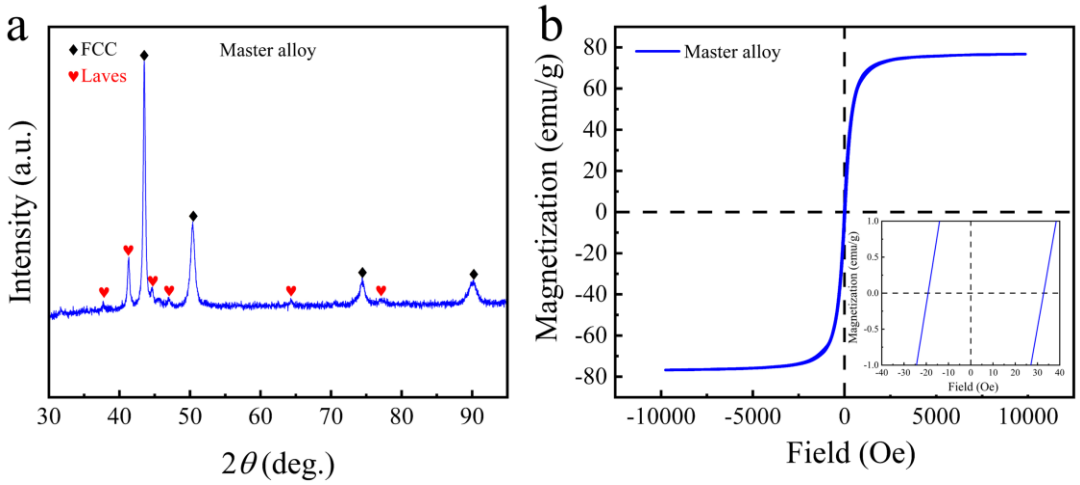

Figure R2. a XRD patterns and **b** magnetic hysteresis loops of $Fe_{34}Co_{29}Ni_{29}Al_3Ta_3Si_2$ master alloy.

(3) The mechanism of **deformation-induced amorphous phase precipitation improving mechanical properties** was first found in HEA fibers.

Therefore, this work would be of great interest to the readership of Nature Communications, and we hope that the modified version of the paper can be satisfactory.

If there are any further suggestions from the reviewer, we would be very delighted to comply with and further improve the work.

Reviewer #3:

Although there are significant publications in the field of high entropy alloys, this paper appears to have made **some publication-worthy contributions to the field**. The authors' strategy was to control the relationship between microstructure, magnetism and the mechanical strength such that coercivity is minimized and tensile strength is maximized. Consequently, soft magnetic fibers of Fe34Co29Ni29Al3Ta3Si2, with good tensile elongation, were produced by in-rotating-water spinning method. To be suitable for publication, especially in Nature Communications, some improvements are needed.

Thanks for the reviewer's recognition of the high quality of our paper. We appreciate the reviewer's helpful and positive comments. We further improved this paper according to the reviewer's excellent suggestions.

Comment 1: The authors seem to have missed the opportunity to discuss their work in view of another work that (perhaps) is the most closely related composition to theirs (DOI: 10.1016/j.intermet.2020.106801). In terms of the constituent elements, the key difference is the use of Ta in the present work. Discussion of the differences in the magnetic properties would have been very insightful.

Response 1: Thanks for the reviewer's good suggestions. Discussion of the differences for this work and previous related composition (DOI: 10.1016/j.intermet.2020.106801) were added in revised manuscript. This work: DOI: 10.1016/j.intermet.2020.106801 was cited as Ref. [26] in the revised manuscript **(lines 75-76, page 4).**

The resultant micron-diameter soft-magnetic HEA fiber has a tensile strength of 674 MPa at 23% elongation, a low coercivity of 8.1 Oe, a moderate magnetization of 116 emu/g at 10 kOe and a high Curie temperature of 770 K. The single-phase $(Co_{30}Fe_{45}Ni_{25})_{0.8}(Al_{40}Si_{60})_{0.2}$ HEA has a combination of high yielding strength of 1636 MPa, relatively-high M_s of 1.24 T, and low H_c of 0.75 Oe [19] . The slightly larger H_c of the as-spun fibers compared to previously reported $(Co_{30}Fe_{45}Ni_{25})_{1-x}(Al_{40}Si_{60})_x$ bulk HEAs is due to the pinning effect of the Ta-rich phase on the movement of the domain wall and the influence of localized stress [19]. **(lines 274-276, page 13-14).**

Modifications: In our revised manuscript, we added the following discussions:

On Page 4 lines 74-79: "*The single-phase $(Co_{30}Fe_{45}Ni_{25})_{0.8}(Al_{40}Si_{60})_{0.2}$ HEA has a combination of high compressive strength of 1636 MPa, relatively-high M_s of 1.24 T, and low H_c of 0.75 Oe [26]. It has been recognized seems that HEAs with high structural disorder, designable crystal structure and variable magnetic properties can balance plasticity and H_c by tuning particle/matrix interfacial coherency stresses to maximize the interaction strength with dislocations and minimize the pinning of magnetic domain walls[11].*"

On Page 13-14 lines 274-276: "*The slightly larger H_c of the as-spun fibers compared to previously reported $(Co_{30}Fe_{45}Ni_{25})_{1-x}(Al_{40}Si_{60})_x$ bulk HEAs is due to the pinning effect of the Ta-rich phase on the movement of the domain wall and the influence of localized stress[26].*"

Comment 2: A statement on example of soft magnetic materials application in which

the fibers can be used would be useful. In many applications, the fibers may still need to be consolidated which affects the resultant properties for a specific application.

Response 2: Thanks for the reviewer's good suggestions. The statements on examples of soft-magnetic fiber applications were added in the Introduction part **(page 3-5).**

Soft-magnetic fibers (SMFs) with low coercivity (H_c), such as Co-based and Fe-based amorphous and polycrystalline fibers, are fundamental materials that serve in sensors, actuators, and electromagnetic shielding devices, etc.[43, 44, 45, 46, 47, 48, 49]. Recently, permalloys and Co/Fe-based SMFs have obtained significant attention owing to their potential applications in geomagnetic navigation, human-computer interaction, and human-like tactile sensing. However, due to limited stretchability, the large-scale production and application of SMFs and related devices still face numerous challenges [8]. With the advancement of flexible electronics and multifunctional components, there is a substantial need for micrometer-scale SMFs capable of enduring tensile, torsional, and shear loads in long-term operations [50, 51]. That is, the fibers necessitate not just exceptional soft magnetic performance but also miniaturization, great tensile strength and plasticity.

In this work, SMFs with nominal compositions $Fe_{34}Co_{29}Ni_{29}Al_3Ta_3Si_2$ (at. %) and a diameter of ~180 μm were fabricated by the one-step in-rotating-water spinning method. The HEA fibers have a good balance of H_c and tensile elongation, outperforming the other SMFs. This work thus ensures the compatibility of mechanical and soft magnetic properties of SMFs under multi-dimensional deformations and high temperatures, facilitating their large-scale production and application in emerging fields

such as wearable electronics, humanoid robots, and intelligent construction.

Modifications: To address this point, we have made the following addition:

On Page 3 lines 51-56: "*Recently, permalloys and Co/Fe-based SMFs have obtained significant attention owing to their potential applications in geomagnetic navigation, human-computer interaction, and human-like tactile sensing. However, due to limited stretchability, the large-scale production and application of SMFs and related devices still face numerous challenges*[8]."

On Page 5 lines 92-94: "*In this work, an in-rotating-water spinning method was first used to achieve micron-diameter SMFs with coarse-grained structure through a short, energy-saving and high-efficiency process*[34, 35]."

On Page 5 lines 99-103: "*This work thus ensures the compatibility of mechanical and soft magnetic properties of SMFs under multi-dimensional deformations and high temperatures, facilitating their large-scale production and application in emerging fields such as wearable electronics, humanoid robots, and intelligent construction.*"

Comment 3: The authors wrote that the Ta-rich phase was substantially reduced or eliminated in the heat-treated samples, compared to the as-cast samples. How could such a change in composition not reflected in the magnetization? The magnetization (emu/g) should be the sum of magnetic moment from the magnetic phases in the materials, normalized by the mass of both magnetic and non-magnetic contents. Some explanation is needed.

Response 3: Thanks for the reviewer's good suggestions. A more detailed discussion on the stability of M_s was added in the revised manuscript **(line 221-227, page 11).**

Modifications: On page 11 lines 221-227: "*The magnetization and H_c are the key parameters of soft magnetic materials [56].The vacancies in 3d atomic orbitals of Fe, Co and Ni atoms contribute to the magnetic moments, and these vacancies will be filled up by the outer shell electrons of Al and Si[57]. The samples exhibit a stable magnetization at 10 kOe (Supplementary Fig. S2) owing to the magnetic exchange interaction from certain atomic ratio. Upon different annealing conditions, the Ta-rich phase occupies only a small fraction (<1.2%), thus having a negligible effect on magnetization.*"

Comment 4: Please describe the direction of the applied magnetic field during magnetic hysteresis measurement: along vs. across the wire length?

Response 4: Each sample for VSM consists of four 3 mm long fibers interlaced at a 45° angle to eliminate demagnetization and magnetic anisotropy. This sentence was added in the revised manuscript **(lines 413-414, page 20).**

Modifications: On page 20 lines 413-414: "*Each sample for VSM consists of four 3 mm long fibers interlaced at a 45° angle to eliminate demagnetization and magnetic anisotropy.*"

Comment 5: It would be helpful if the rationale for selecting this heat treatment condition were stated.

Response 5: The properties of soft magnetic fibers are different under different annealing conditions. We found that the comprehensive performance obtained by annealing at 800 °C is the best. Therefore, we chose annealing at 800 °C and different times as the focus of our research. For example, the magnetic and mechanical properties of the samples annealed at different temperatures for 1 hour are shown in Fig. R3 a and

b, respectively. The coercivity obtained at 800 °C is the smallest, and both high strength and large plasticity can be obtained at the same time.

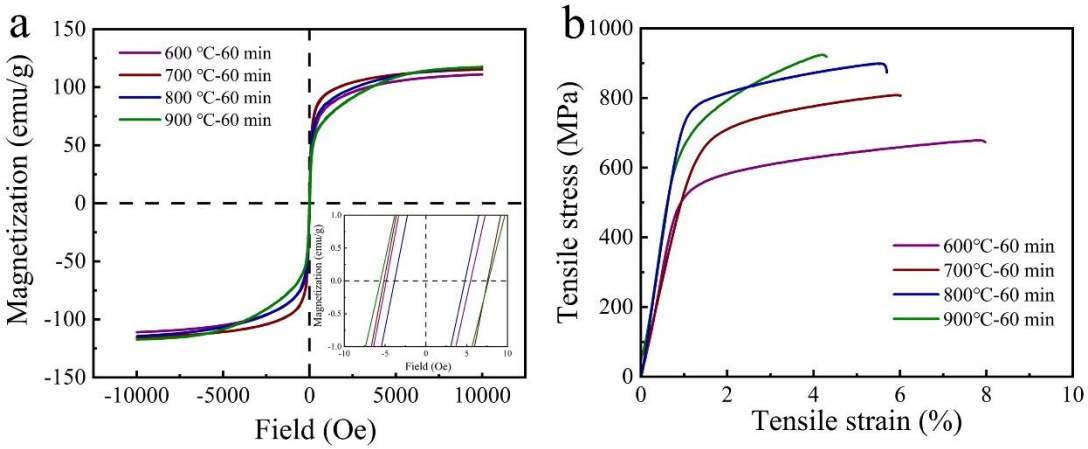

Figure R3. a Magnetic hysteresis loops and **b** tensile engineering stress-strain curves of HEA fibers with different annealing temperature.

Comment 6: It would also be helpful to understand why the authors have not discussed all the other samples made.

Response 6: Thanks for the reviewer's good suggestions. The soft magnetic and mechanical properties of all the samples are shown in Fig. S2 and S4. As the annealing time increases, there is no significant change in magnetization (~116 emu/g at 10 kOe). The H_c of HEA fibers significantly decrease from 8.1 Oe in the as-spun sample to 2.7 Oe in 800 °C-120 min annealed samples, and then slowly decrease to 1.1 Oe in the 300 min-annealed sample (Supplementary Fig. S2). The ultimate tensile strength (σ_u) and fracture elongation (ε_f) of the as-spun sample are 674 MPa and 23.4 %, respectively. The 800 °C-10 min annealed sample shows a good combination of tensile strength (σ_u=835 MPa) and fracture elongation (ε_f=9.9%). The σ_u for the 800 °C-120 min annealed sample reaches 1029 MPa at a cost of the plasticity of ~20 %. The yield strength increased significantly with increased annealing temperature, while plasticity

deteriorated obviously (Supplementary Fig. S4).

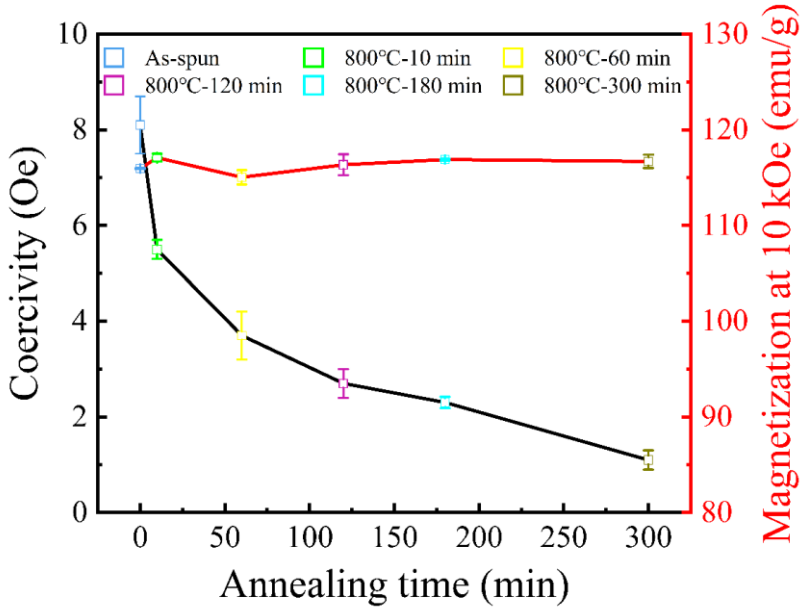

Figure S2. Annealing time dependence of M_s and H_c of HEA fibers.

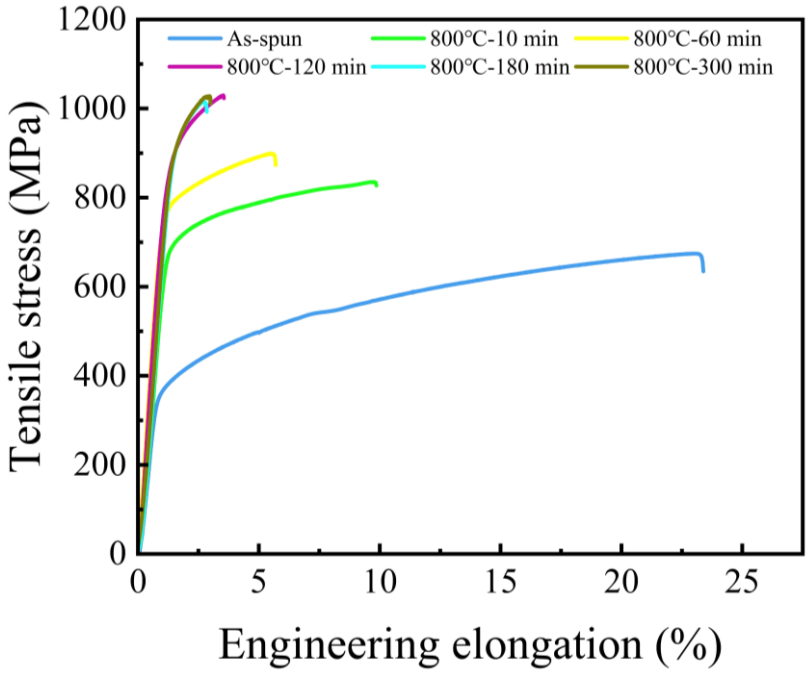

Figure S4. Tensile stress-strain curves of HEA fibers with different annealing time.

Based on the above results, the results of SEM, TEM, Lorentz TEM and 3DAP, which are used for structural characterization and mechanism analysis, only two typical and representative samples were selected, namely, the as-spun sample and the sample

annealed for 120 minutes.

Modifications: On page 6 lines 114-127: *"As the annealing time increases, there is no significant change in magnetization (~116 emu/g at 10 kOe). The H_c of HEA fibers significantly decrease from 8.1 Oe in the as-spun sample to 2.7 Oe in the 800 ℃-120 min annealed sample, and then slowly decrease to 1.1 Oe in the 300 min-annealed sample (Supplementary Fig. S2). The Curie temperature of the as-spun and 800 ℃-120 min annealed samples are 770 and 690 K, respectively (Supplementary Fig. S3), indicating the excellent high-temperature tolerance of the alloys. Fig. 1e presents the tensile stress-strain curves of the HEA fibers at different states. The ultimate tensile strength (σ_u) and fracture elongation (ε_f) of the as-spun sample are 674 MPa and 23.4 %, respectively. The 800 ℃-10 min annealed sample shows a good combination of tensile strength (σ_u=835 MPa) and fracture elongation (ε_f=9.9%). The σ_u for the 800 ℃-120 min annealed sample reaches 1029 MPa at a cost of the plasticity of ~20 %. The yield strength increased significantly with increased annealing temperature, while plasticity deteriorated obviously (Supplementary Fig. S4)."*

Comment 7: Since the hysteresis plots were not saturated, saturation magnetization (Ms) should not be used. Consider M@10kOe.

Response 7: Thanks for the reviewer's good suggestion. The corresponding contents "saturation magnetization (Ms)" have been replaced by "M at 10 kOe" in revised manuscript.

Modifications: On page 2 lines 41: *"magnetization of 116 emu/g at 10 kOe";*

On page 6 lines 115: *"magnetization (~116 emu/g at 10 kOe)"*

Comment 8: On the First line of the Microstructure analysis section: please identify the "small peak" with its 2theta position.

Response 8: The "small peak (2θ=50.81°)" was provided in the first line of the Microstructure analysis section. **(lines 145-146, page 7).**

Modifications: On page 7 lines 145-146: "*The small peak (2θ=50.81°) detected in the 800 °C-120 min annealed HEA fibers besides the FCC (200) peak corresponds to the $L1_2$ structure.*"

Comment 9: Why is the discussion on the role of the Ta-rich phase missing in the Deformation Mechanism section?

Response 9: The authors appreciate your comments a lot. The Ta-rich phase identified in the present work ($Ta_2(Co/Fe/Ni)_3Si$, space group: 194#, a=4.8 Å, c=7.6 Å) is in fact highly similar to the well-studied $(Co/Fe)_2Ta$ type Laves phase (space group: 194#, a=4.797 Å, c=7.827 Å) in FCC HEAs[52]. They possess the same crystalline structure, approximate lattice constants, and same content of Ta in unit cell (1/3). Our HAADF-STEM EDS results confirm the chemical composition of the Laves-like phase as shown in Fig. R4a. The Laves phase is known as a hard yet brittle phase at ambient temperature, which contributes to the yield strength by blocking dislocations[53]. The reasons for the absence of the discussion on the role of the Ta-rich phase in response to deformation are as follows: First, the as-spun HEA fibers show a negligible volume fraction of $Ta_2(Co/Fe/Ni)_3Si$ phase, ~1.2% according to our determination from TEM observation. This value is consistent with that in a $CoCrFeNiTa_{0.1}$ HEA with similar Ta content (2.4

at.%), which has a Laves volume fraction of 0.97%[54]. Such a volume fraction contribute little (only ~10 MPa determined according to Ref. [55]) to the mechanical properties of HEAs. Moreover, the Ta-rich Laves phases are hard and brittle, they can block dislocations and serve as nanovoid initiation sites during deformation[53, 56]. Our TEM observation also revealed the dislocation pile-ups and nanovoids around the $Ta_2(Co/Fe/Ni)_3Si$ particle in the deformed as-spun HEA fiber, as shown in Fig. R4b. Thanks to this comment, we have added a discussion on the deformation of Ta-rich phase in the revised manuscript **(lines 341-345, page 17)**. The deformed morphology of the $Ta_2(Co/Fe/Ni)_3Si$ phase was added in the Supplementary Materials.

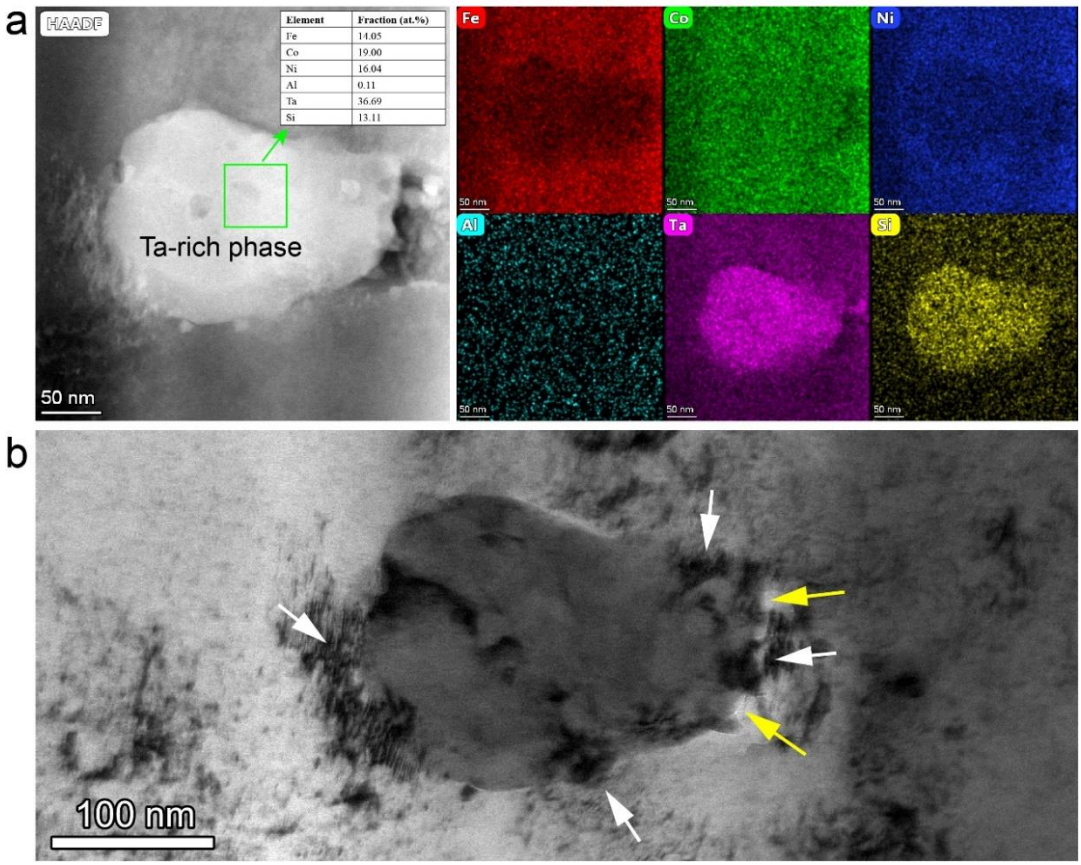

Figure. R4. a HAADF-STEM EDS results showing the elemental distribution of the Ta-rich phase in the as-spun HEA fiber. Inset is the chemical compositions of the area framed by a green box. **b** TEM observation of a $(Ta_2(Co/Fe/Ni)_3Si$ particle in the as-spun HEA fiber after deformation, where dislocation pile-ups are indicated by white arrows, micro-voids are indicated by yellow arrows.

Modifications: On page 17 lines 341-345: "*Regarding the $Ta_2(Co/Fe/Ni)_3Si$ particles, our observations show that they act as dislocation accumulation and nanovoid nucleation sites during deformation (see Supplementary Fig. S12). Since the volume fraction of the $Ta_2(Co/Fe/Ni)_3Si$ particles in the as-spun HEA fibers is only 1.2 %, their contribution to the mechanical properties is negligible.*"

Comment 10: There are some terms introduced without definition. For example, TEM and 3D-APT, etc.

Response 10: Thanks for the reviewer's helpful comment. The transmission electron microscopy (TEM) and three-dimensional atom probe tomography (3D APT) were defined in the revise manuscript. **(page 8, line 155 and page 9, line 185).**

Modifications: On page 8 lines 155: *"The transmission electron microscopy (TEM) characterizations were further carried out";*

On page 9 lines 185: *"Fig. 3a, b and c display the three-dimensional atom probe tomography (3D APT) results of FCC matrix of the as-spun fibers.";*

Comment 11: There are several typographical errors in the manuscript that need to be addressed. These are some examples:

(1) "reorganized" on page 4 should be "recognized";

(2) A sentence that started with "it" on page 4 should be "It";

(3) The indefinite article "an" in line 5 of the Result and Discussion section should be "a";

(4) First line of the Microstructure analysis section: "were" should be "was";

(5) The preposition "to" is missing in line 7 of First line of the Microstructure analysis

section.

(6) On line 2 of the “Deformation mechanism” section, is “rational” the correct word?

(7) Please check these sentences:

Page 17: “To reduce the impact of the grip on the specimens, a layer of cardboard was covered.”

Page 18: The grain morphology of the samples was characterized via electron backscatter diffraction (EBSD) was performed in a SEM (Verios G4 UC, Thermo Fisher Scientific).

Response 11: Thanks for the reviewer’s helpful comments. The English grammar and the expressions were checked point by point to avoid mistakes by authors. Besides, our good English colleagues have also helped us checking and editing the language of full manuscript. Some specific errors pointed out by reviewer were revised as follows:

(1) “reorganized” on page 4 lines 76 was replaced by “recognized”;

(2) A sentence that started with “it” on page 4 lines 86 was replaced by “It”;

(3) The indefinite article “an” on page 5 lines 109 of the Result and Discussion section was replaced by “a”;

(4) On page 7 lines 142, first line of the Microstructure analysis section: “were” was replaced by “was”;

(5) The “to” was added on page 7 line 149 of First line of the Microstructure analysis section;

(6) On page 14 lines 289 of the “Deformation mechanism” section, the “rational” was corrected as “radial”;

(7) The sentences: “To reduce the impact of the grip on the specimens, a layer of cardboard was covered.” was rewritten as “In order to mitigate the effect of handling on the samples, a protective layer of cardboard was utilized.” on page 21 lines 421-423;

The sentences: “The grain morphology of the samples was characterized via electron backscatter diffraction (EBSD) was performed in a SEM (Verios G4 UC, Thermo Fisher Scientific)” was rewritten as “The morphological analysis of the grains within the samples was conducted through electron backscatter diffraction (EBSD) in the SEM (Verios G4 UC, Thermo Fisher Scientific).” on page 21 lines 436-438.

Thank you again very much for your valuable comments and suggestions.

References

1. Sun Q-C, *et al.* Magnetic domains and domain wall pinning in atomically thin $CrBr_3$ revealed by nanoscale imaging. *Nat. Commun.* **12**, 1989 (2021).

2. Willard M, Daniil M. Chapter Four - Nanocrystalline soft magnetic alloys two decades of progress. In: *Handbook of Magnetic Materials* (ed Buschow KHJ). Elsevier (2013).

3. Li Z, *et al.* Strength, plasticity and coercivity tradeoff in soft magnetic high-entropy alloys by multiple coherent interfaces. *Acta Mater.* **254**, 118970 (2023).

4. Michael, *et al.* Amorphous and nanocrystalline materials for applications as soft magnets. *Prog. Mater. Sci.* **40,** 333-407 (1999).

5. Li H, Lu Z, Wang S, Wu Y, Lu Z. Fe-based bulk metallic glasses: glass formation, fabrication, properties and applications. *Prog. Mater. Sci.* **103**, 235-318 (2019).

6. Han L, *et al.* A mechanically strong and ductile soft magnet with extremely low coercivity. *Nature* **608**, 310-316 (2022).

7. Han L, *et al.* Ultrastrong and ductile soft magnetic high-entropy alloys via coherent ordered nanoprecipitates. *Adv. Mater.* **33**, 2102139 (2021).

8. Yang H, *et al.* Advances in flexible magnetosensitive materials and devices for wearable electronics. *Adv. Mater.* **2311996**,1-33 (2024).

9. Yeh J, *et al.* Nanostructured high-entropy alloys with multiple principal elements: novel alloy design concepts and outcomes. *Adv. Eng. Mater.* **6**, 299-303 (2004).

10. Cantor B, Chang I, Knight P, Vincent A. Microstructural development in equiatomic multicomponent alloys. *Mat. Sci. Eng. A* **375-377**, 213-218 (2004).

11. Liu D, *et al.* Exceptional fracture toughness of CrCoNi-based medium and high-entropy alloys at 20 kelvin. *Science* **378**, 978-983 (2022).

12. Gludovatz B, Hohenwarter A, Catoor D, Chang E, George E, Ritchie R. A fracture-resistant high-entropy alloy for cryogenic applications. *Science* **345**, 1153-1158 (2014).

13. Zhang C, *et al.* Strong and ductile FeNiCoAl-based high-entropy alloys for cryogenic to elevated temperature multifunctional applications. *Acta Mater.* **242**,118449 (2022).

14. Gou S, *et al.* Additive manufacturing of ductile refractory high-entropy alloys via phase engineering. *Acta Mater.* **248**, 118781 (2023).

15. Jo Y, *et al.* Cryogenic strength improvement by utilizing room-temperature deformation twinning in a partially recrystallized VCrMnFeCoNi high-entropy alloy. *Nat. Commun.* **8**, 15719 (2017).

16. Chaudhary V, Chaudhary R, Banerjee R, Ramanujan R. Accelerated and conventional development of magnetic high entropy alloys. *Mater. Today* **49**, 231-252 (2021).

17. Zhang J, *et al.* Native oxidation and complex magnetic anisotropy-dominated soft magnetic CoCrFeNi-based high-entropy alloy thin films. *Adv. Sci.* **9**, 2203139 (2022).

18. Orbay Y, Rao Z, Çakır A, Tavşanoğlu T, Farle M, Acet M. Magnetic properties of the FCC and BCC phases of $(MnFeCoNi)_{80}Cu_{20-x}Z_x$ (Z: Al, Ga) high-entropy alloys. *Acta Mater.* **259**, 119240 (2023).

19. Zhou K, *et al.* FeCoNiAlSi high entropy alloys with exceptional fundamental and application-oriented magnetism. *Intermetallics* **122**, 106801 (2020).

20. Herzer G. Modern soft magnets: amorphous and nanocrystalline materials. *Acta Mater.* **61**, 718-734 (2013).

21. Jia Y, *et al.* Efficient coarse-grained superplasticity of a gigapascal lightweight refractory medium entropy alloy. *Adv. Sci.* **2207535**, 1-12 (2023).

22. Ochin P, *et al.* Shape memory thin round wires produced by the in rotating water melt-spinning technique. *Acta Mater.* **54**, 1877-1885 (2006).

23. Inoue A, Hagiwara M, Masumoto T. Production of Fe-P-C amorphous wires by in-rotating-water spinning method and mechanical-properties of the wires. *J. Mater. Sci.* **17**, 580-588 (1982).

24. Wei D, *et al.* Si-addition contributes to overcoming the strength-ductility trade-off in high-entropy alloys. *Int. J. Plast.* **159**, 103443 (2022).

25. Zhang Y, Zuo T, Cheng Y, Liaw P. High-entropy alloys with high saturation magnetization, electrical resistivity and malleability. *Sci. Rep.* **3**, 1455 (2013).

26. Yang T, *et al.* Multicomponent intermetallic nanoparticles and superb mechanical behaviors of complex alloys. *Science* **362**, 933-937 (2018).

27. He J, *et al.* A precipitation-hardened high-entropy alloy with outstanding tensile properties. *Acta Mater.* **102**, 187-196 (2016).

28. Fan L, *et al.* Ultrahigh strength and ductility in newly developed materials with coherent nanolamellar architectures. *Nat. Commun.* **11**, 6240 (2020).

29. Zhao Y, *et al.* Development of high-strength Co-free high-entropy alloys hardened by nanosized precipitates. *Scripta Mater.* **148**, 51-55 (2018).

30. Qi W, *et al.* Effects of Ta microalloying on the microstructure and mechanical properties of $L1_2$-strengthened CoCrFeNi–AlTi high-entropy alloys. *Mat. Sci. Eng. A* **875**, 145048 (2023).

31. Mitera M, Naka M, Masumoto T, Kazama N, Watanabe K. Effects of metalloids on the magnetic properties of iron based amorphous alloys. *Phy. Status Solidi A* **49**, K163-K166 (1978).

32. Xue Q, Cerreta E, Grayiii G. Microstructural characteristics of post-shear localization in cold-rolled 316L stainless steel. *Acta Mater.* **55**, 691-704 (2007).

33. Zhao S, *et al.* Amorphization in extreme deformation of the CrMnFeCoNi high-entropy alloy. *Sci. Adv.* **7**, eabb3108 (2021).

34. Ming K, Lu W, Li Z, Bi X, Wang J. Amorphous bands induced by low temperature tension in a non-equiatomic CrMnFeCoNi alloy. *Acta Mater.* **188**, 354-365 (2020).

35. Han S, Zhao L, Jiang Q, Lian J. Deformation-induced localized solid-state amorphization in nanocrystalline nickel. *Sci. Rep.* **2**, 493 (2012).

36. Gratz A, Deloach L, Clough T, Nellis W. Shock amorphization of cristobalite. *Science* **259**, 663-666 (1993).

37. Subhash G, Awasthi A, Kunka C, Jannotti P, Devries M. In search of amorphization-resistant boron carbide. *Scripta Mater.* **123**, 158-162 (2016).

38. Ovid'ko I. Nanoscale amorphization as a special deformation mode in nanowires. *Scripta Mater.* **66**, 402-405 (2012).

39. Wang H, *et al.* Deformation-induced crystalline-to-amorphous phase transformation in a CrMnFeCoNi high-entropy alloy. *Sci. Adv.* **7**, eabe3105 (2021).

40. Wu W, Ni S, Liu Y, Liu B, Song M. Amorphization at twin-twin intersected region in FeCoCrNi high-entropy alloy subjected to high-pressure torsion. *Mater. Charact.* **127**, 111-115 (2017).

41. Jiang K, *et al.* Abnormal hardening and amorphization in an FCC high entropy alloy under extreme uniaxial tension. *Int. J. Plast.* **159**, 103463 (2022).

42. Bu Y, *et al.* Elastic strain-induced amorphization in high-entropy alloys. *Nat. Commun.* **15**, 4599 (2024).

43. Charles A, Rider A, Brown S, Wang C. Multifunctional magneto-polymer matrix composites for electromagnetic interference suppression, sensors and actuators. *Prog. Mater. Sci.* **115**, 100705 (2021).

44. Feng T, *et al.* Real-time self-monitoring and smart bend recognizing of fiber-reinforced polymer composites enabled by embedded magnetic fibers. *Compos. Sci. Technol.* **232**, 109869 (2023).

45. Qin F, Peng H. Ferromagnetic microwires enabled multifunctional composite materials. *Prog. Mater. Sci.* **58**, 183-259 (2013).

46. Pei C, *et al.* Superlattice-shelled nanocrystalline core structural design for highly sensitive GMI sensors. *Acta Mater.* **255**, 119088 (2023).

47. Chiriac H, Óvári T. Amorphous glass-covered magnetic wires: preparation, properties, applications. *Prog. Mater. Sci.* **40**, 333-407 (1996).

48. Jurc R, *et al.* 28 - Sensoric application of glass-coated magnetic microwires. In: *Magnetic Nano- and Microwires (Second Edition)* (ed Vázquez M). Woodhead Publishing (2020).

49. Zhukov A, Ipatov M, Corte-Leon P, Blanco J, Zhukova V. Advanced magnetic microwires for sensing applications. In: *Encyclopedia of Materials: Electronics* (ed Haseeb ASMA). Academic Press (2023).

50. Xiao H, *et al.* Dual mode strain–temperature sensor with high stimuli discriminability and resolution for smart wearables. *Adv. Funct. Mater.* **33**, 2214907 (2023).

51. Zhang Y, Gan T, Dong J, Liu Q, Wang J, Shi W. Enhanced magnetoimpedance effect of carbon fiber/Fe-based alloy coaxial composite by tensile stress. *Carbon* **93**, 451-457 (2015).

52. Ai C, *et al.* Effect of Ta addition on solidification characteristics of $CoCrFeNiTa_x$ eutectic high entropy alloys. *Intermetallics* **120**, 106769 (2020).

53. Liu T, Chen D, Gao X, Qin G, Chen R. Microstructure and strengthening mechanisms in multi-phase $Ni_{36}Co_{30}Cr_{11}Fe_{11}Al_{12-x}Ta_x$ high entropy alloy. *Mater. Charact.* **214**, 114105 (2024).

54. Li A, *et al.* Effect of C content on microstructure evolution and mechanical properties of $CoCrFeNiTa_{0.1}$ high entropy alloy. *J. Alloy. Compd.* **1002**, 175138 (2024).

55. Li J, *et al.* The microstructure and mechanical properties of novel Fe-rich Fe–Cr–Ni–Ta eutectic multi-principal element alloys. *J. Mater. Sci. Technol.* **26**, 7273-7283 (2023).

56. Wang J, *et al.* Coupling effects of temperature and strain rate on the mechanical behavior and microstructure evolution of a powder-plasma-arc additive manufactured high-entropy alloy with multi-heterogeneous microstructures. *Acta Mater.* **276**, 120147 (2024).

Review Report

In "**A one-step fabricated soft magnetic high entropy alloy fibre with excellent strength and flexibility"** by **Yan Ma et. al**., the authors fabricated soft magnetic HEA alloy micron-sized wires with tailored mechanical properties which is quite impressive. It is a well-executed study that makes a valuable contribution to the field of material science. The author has provided a thorough explanation and rationale for the formation of Fe34Co29Ni29Al3Ta3Si2 high entropy alloy (HEA) fibre. The research addresses a critical and underexplored problem in synthesis of large micron-sized soft magnetic fibers, providing insights into dislocation proximity, plasticity, the domain wall pinning and coarsening of grains leading to the formation of low coercivity multicomponent flexible wires. The results presented are clear and in logical manner, effectively supporting the stated hypotheses.

The authors have well described the ***beneficial mechanisms of magnetization and mechanical properties of fabricated micron-sized HEA fibers carried out through magnetic and microstructure analyses.*** Minor revisions are recommended to refine the manuscript which are as follows:

1. In page 2, line no. 61, it has been written that the first introduction of high entropy alloys (HEAs) was in **2002,** but it was in **2004** as per references mentioned. Ref [18] by Ma et. al. was on bulk metallic glasses only.
2. A point defect can pin magnetic domains (Magnetic domains and domain wall pinning in atomically thin $CrBr_3$ revealed by nanoscale imaging, Nature Communications, 12 (2021), 1989). Not pinning of magnetic wall domains by nanocrystalline $L1_2$ precipitates needs further scientific verifications and discussions. May be the coherency and not the size helped in the not-pinning process.
3. The readers would find it more relatable if the JCPDS data used for phase identification and peak matching in XRD were also mentioned.